# NANOCRYSTALLINE S304H AUSTENITIC STAINLESS STEEL PROCESSED BY MULTIPLE FORGING

**M. Tikhonova, Y. Kuzminova, A. Belyakov and R. Kaibyshev**

Belgorod State University, Pobeda 85, Belgorod 308015, Russia

**Abstract.** A Super304H austenitic stainless steel, Fe – 0.1%C – 0.12%N – 0.1%Si – 0.95%Mn – 18.4%Cr – 7.85%Ni – 3.2%Cu – 0.5%Nb – 0.01%P – 0.006%S (all in mass%), with an average grain size of about 10 μm was used as the starting material. The multiple forging was carried out by means of multi-pass compressions at room temperature. The hardness of 6 GPa and the yield strength of 1430 MPa were achieved after total strain of 4. The strengthening during the multiple forging resulted from the formation of almost equiaxed nanocrystalline structure with an average grain size of about 30 nm. The softening behaviour of the nanocrystalline samples was studied by means of isochronal annealing at temperatures of 500 to 700 °C for 30 min. The structural mechanisms responsible for the grain refinement during the large strain cold working and those operating upon the subsequent annealing and their effect on the mechanical properties are considered.

## 1. INTRODUCTION

Severe plastic deformation that is large strain cold working at temperatures below about half of melting point is now considered as one of efficient method for the development of submicro- or nanocrystalline metals and alloys [1,2]. The total strains required for the development of deformation microstructures consisting of highly misoriented structural elements with their size in the range of tens to hundred nanometers are significantly larger than those used in conventional metal working processes [3-5]. Recently, several research centres around the world have developed and practically utilized several processing techniques, which allowed deforming various metals and alloys up to very large strains at relatively low temperatures including severe deformation at room temperature. The most widespread and universal techniques are mechanical milling/alloying with subsequent consolidation, equal channel angular pressing, torsion under high pressure, accumulative roll bonding [6-14].

Early investigations revealed the common sequence of structural changes leading to the grain refinement during severe deformation. The development of submicro- or nanocrystalline structures results from a kind of continuous reactions [9]. The plastic working brings about a spatial network of deformation subboundaries. Then, the new fine grains are gradually evolved in place of deformation subgrains as a result of progressive increase in the subboundary misorientations with straining. It should be noted that various metals and alloys are characterized by remarkably different kinetics of grain refinement during severe deformation [15-18]. The rapid development of nano/submicrocrystalline structures was observed in materials allowing pronounced grain subdivision upon deformation. Typical representatives of such materials are titanium alloys and metastable austenitic steels [19-21]. The grain refinement in these materials is accelerated by multiple mechanical twinning and/or strain-induced phase transformation, leading to fast development of nano/submicrocrystalline structures at relatively small

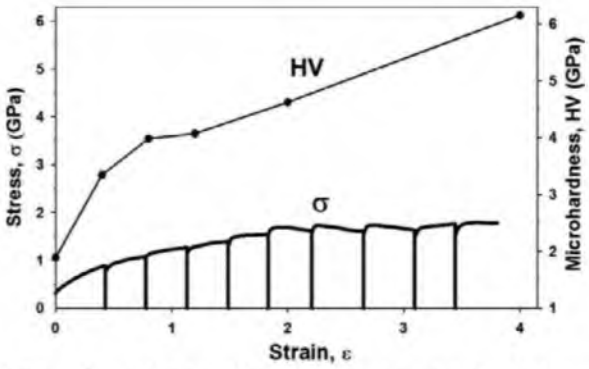


**Fig. 1.** Stress-strain curves and strain-microhardness during multiple forging of a 304-type austenitic stainless steel.

strains, which can be easily attained by ordinary metal working processes. The aim of present study is to investigate a feasibility of nanostructurization of an austenitic stainless steel during multiple forging at an ambient temperature. The study is focussed on the quantitative clarification of structural changes during cold working and subsequent annealing.

## 2. EXPERIMENTAL PROCEDURE

A Super304H austenitic stainless steel, Fe – 0.1%C – 0.12%N – 0.1%Si – 0.95%Mn – 18.4%Cr – 7.85%Ni – 3.2%Cu – 0.5%Nb – 0.01%P – 0.006%S (all in mass%), was used as the starting material. The steel forgings were solution treated at 1100 °C for 30 min followed by air cooling. The average grain size was about 10 μm. Rectangular samples with initial dimension of 10 × 12 × 15 $mm^3$ were cut for multiple forging tests. The multiple forging was carried out by means of multi-pass compression tests with a change of the loading direction in 90° in order of three orthogonal axes at room temperature. The samples were compressed under a strain rate of $10^{-3}$ $s^{-1}$ to a strain of ~0.4 in each pass. The samples processed to a total strain of 4 were annealed at temperature 500, 600, 700 °C for 30 min. The structural characterization was carried out on the sample sections parallel to the compression axis in the last pass by using an optical microscope, a Jeol JEM-2100 transmission electron microscope and a Quanta 600F scanning electron microscope equipped with an electron back scattering diffraction (EBSD) analyser incorporating an orientation imaging microscopy (OIM) system. Besides the EBSD technique, the phase content, i.e. austenite/ferrite fraction, was evaluated by a method of magnetic force microscopy (MFM) using an INTEGRA Aura atomic force microscope and by X-ray analysis using a Rigaku Ultima IV diffractometer. The mechanical properties at room temperature were studied in tension by using the specimens with a 12 mm gauge length and 3.0×1.5 $mm^2$ cross section. An Instron 5882 machine was used.

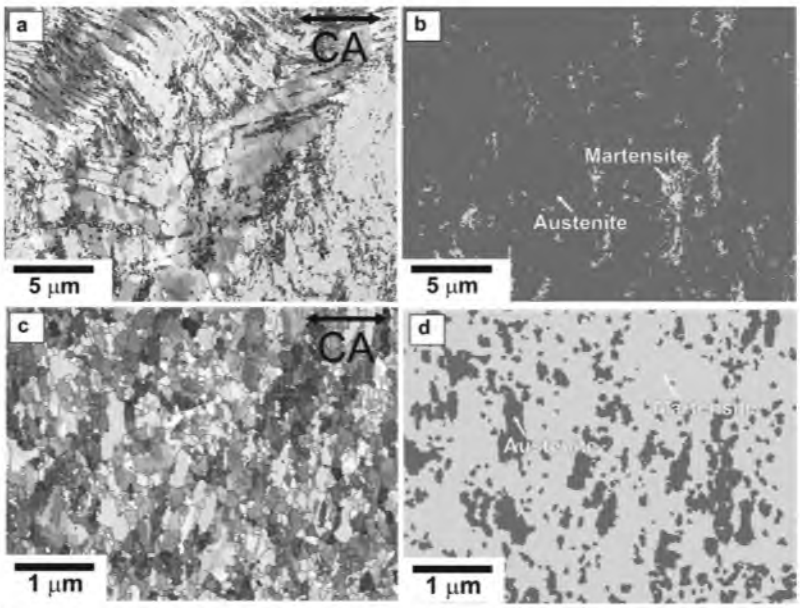


**Fig. 2.** Typical OIM pictures of deformation microstructures in a 304-type austenitic stainless steel after multiple forging to strains of $\varepsilon = 0.8$ (a,b) and $\varepsilon = 4$ (c,d). The white and black lines in (a) and (c) correspond to low-angle and high angle boundaries with misorientations of $2° \leq \theta < 15°$ and $15° \leq \theta$, respectively. The distributions of austenite and ferrite grains are represented in (b) and (d) for the same areas shown in (a) and (c), respectively.

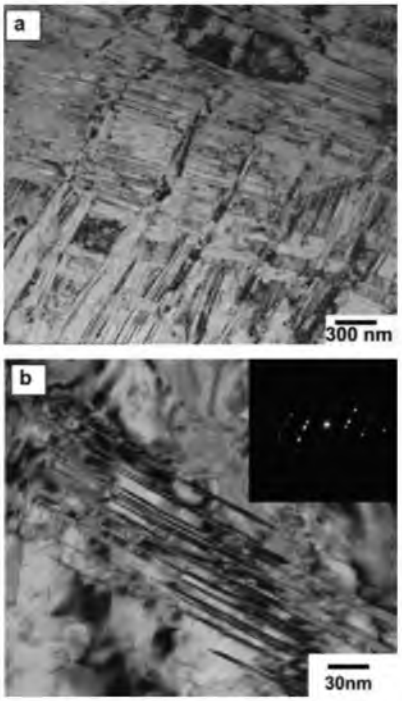


**Fig. 3.** Typical TEM pictures of a 304-type austenitic stainless steel after multiple forging to a strain of $\varepsilon = 0.8$.

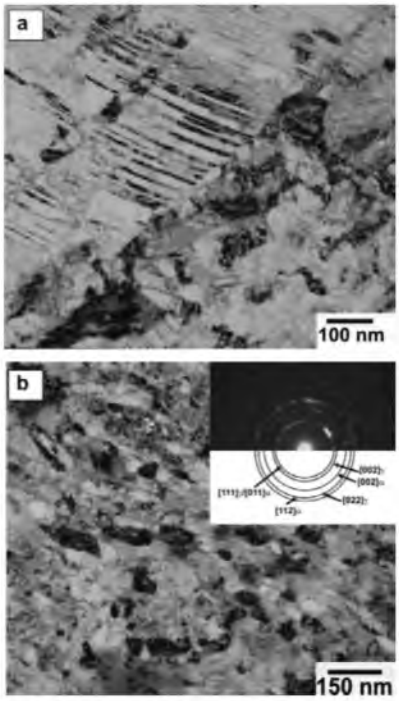


**Fig. 4.** Typical TEM pictures of a 304-type austenitic stainless steel after multiple forging to strains of $\varepsilon = 2$ (a) and $\varepsilon = 4$ (b).

## 3. RESULTS AND DISCUSSION

### 3.1. Strain hardening

A series of the true stress-true strain curves plotted for ten sequential forging passes are shown in Fig. 1 along with a hardness measured on some specimens processed to various strains. The multiple cold forging is accompanied by a significant strain hardening. The most pronounced hardening takes place during the two first forging passes, when the flow stress increases in two times and the hardness is trebled. Upon further multiple deformation the rate of strain hardening decreases. The flow stress approaches its saturation on the level about 1.6 GPa after five forging passes. In contrast, the hardness tends to increase even in large strains and finally attains the level above 6 GPa.

### 3.2. Deformation microstructures

Typical deformation microstructures evolved in the steel after multiple forging to total strains of 0.8 and 4.0 are shown in Fig. 2. The inhomogeneous microstructure consisting of deformation twins and deformation microbands are evolved after two forging passes (Fig. 2a). Since the austenite in the studied steel is metastable at room temperature, the cold working is accompanied by the martensitic transformation. The deformation martensite starts to appear mainly along the deformation twins and deformation microbands, where the deformation inhomogeneities are rapidly developed (Fig. 2b). The multiple forging to large total strains promotes the development of uniform microstructure that is composed of equiaxed fine grains (Fig. 1c). The both austenite and ferrite grains can be clearly recognised in the microstructure (Fig. 1d). Therefore, a kind of duplex microstructure develops after ten forging passes.

Representative TEM fine structures that evolved in the steel during the multiple forging to different strains are shown in Figs. 3 and 4. It is clearly seen in Fig. 3 that the main mechanism of grain subdivision at relatively small strains is associated with the multiple mechanical twinning, which leads to the appearance of nanoscale structural elements outlined by high-angle boundaries. The subsequent change in the loading direction assists the formation of mutually crossed twins and, therefore, results in the development of spatial network of high-angle boundaries of deformation origin. It should be noted that the mechanical twinning continues to operate in austenite even at large strains (Fig. 4a). The inter-boundary spacing in some austenite grains, which are subdivided by twins, can be less than 10 nm. The deformation microstructure that evolved after the final forging pass is composed of alternating nano-scale austenite and ferrite grains (Fig. 4b). The

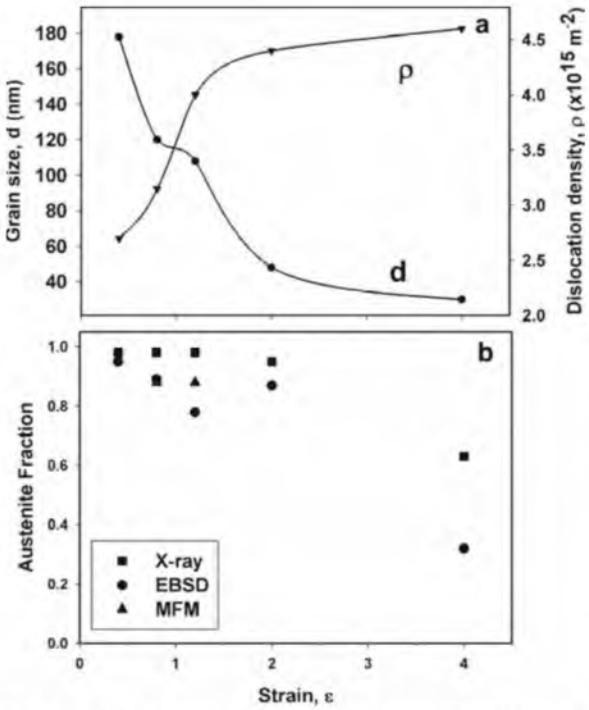


**Fig. 5.** Strain dependencies of the grain size and the dislocation density (a), and the austenite fraction (b) for a 304-type austenitic stainless steel processed by cold multiple forging.

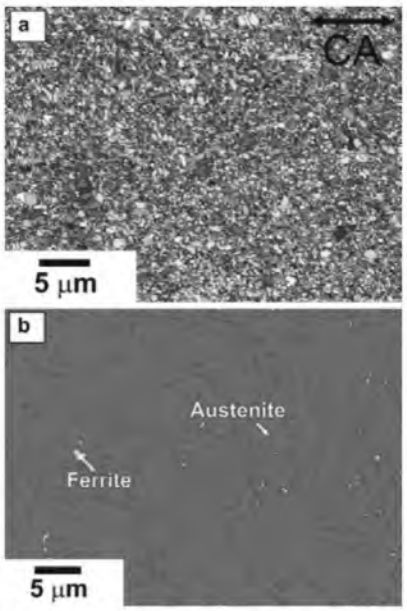


**Fig. 6.** Typical OIM pictures of a 304-type austenitic stainless steel after multiple forging to a strain of $\varepsilon = 4$ and annealing for 30 min at 700 °C. White and black lines in (a) correspond to low-angle and high-angle boundaries with misorientations of $2° \leq \theta < 15°$ and $15° \leq \theta$, respectively. The distribution of austenite and ferrite is represented in (b).

both of them are similar in appearance; they are almost equiaxed and the same in their mean size of about 30 nm.

Fig. 5 represents the quantitative effect of forging strain on some microstructural parameters. The grain size rapidly decreases to about 50 nm during the deformation to a total strain of 2. Then, the rate of grain refinement decreases; the mean grain size gradually approaches 30 nm after the ten sequential forging passes. The change in the dislocation density clearly correlates with the strain dependence of the deformation grain size. Namely, following the rapid increase of the dislocation density during the two first forging passes, the dislocation density approaches its saturation of about $4.5 \times 10^{15}$ m$^{-2}$ in large strains. The plastic working is accompanied by strain-induced martensitic transformation. The austenite fraction slightly changed in the strain range of 0 to 2, whereas further deformation to a strain of 4 leads to decrease in the austenite fraction to about 0.4.

## 3.3. Annealing behaviour

The most important mechanism of structural changes during the heating of the processed steel is the austenite reversion. Fig. 6 shows a typical microstructure evolved in the steel by 30 min annealing at 700 °C. The annealed microstructure is almost fully composed of equiaxed austenite grains. A small amount of ferrite grains is uniformly distributed throughout. The effect of annealing temperature on the structural changes is illustrated in Figs. 7 and 8. Annealing at temperatures below 600 °C does not led to remarkable changes in the deformation microstructure. The mean grain size and the dislocation density remain almost unchanged. An increase in the annealing temperature results in near threefold decrease in the dislocation density. The grain size hardly increases during annealing at 600 °C, while a remarkable grain coarsening takes place upon heating to higher temperatures. An example of the annealed austenite grain evolved after the heat treatment at 700 °C is shown in the right bottom portion of Fig. 7c. This dislocation-free grain grows out consuming work hardened surroundings. Therefore, a discontinuous static recrystallization follows the austenite reversion in the cold worked steel during annealing at temperatures above 600 °C.

## 3.4. Tensile behaviour.

The engineering stress-engineering strain curves obtained during the tensile tests of the cold worked

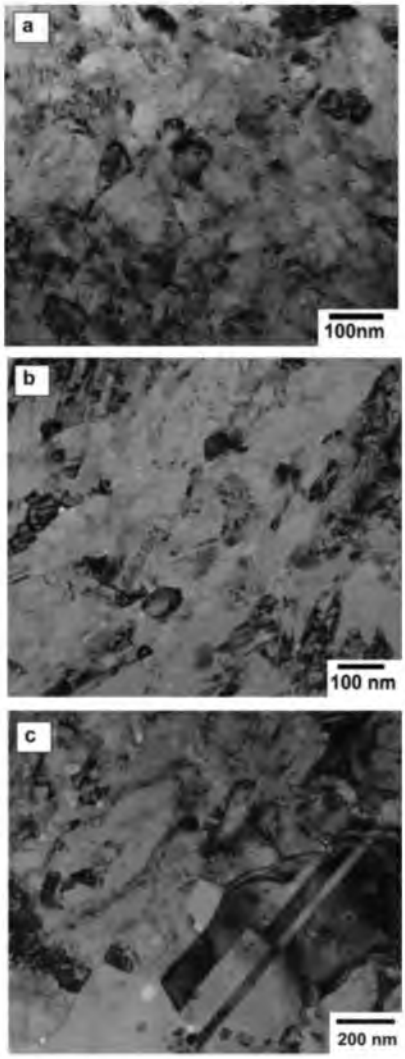


**Fig. 7.** Typical annealed microstructures developed in a 304-type austenitic stainless steel, which was multiple forged to a strain of 4.0 and then annealed for 30 min at different temperatures; (a) $T$ = 500 °C, (b) $T$ = 600 °C, (c) $T$ = 700 °C.

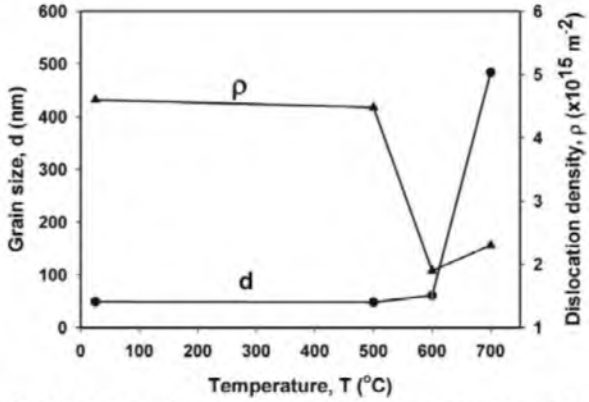


**Fig. 8.** Effect of annealing temperature on the grain size and the dislocation density in a 304-type austenitic stainless steel subjected to multiple forging to a total strain of 4.0.

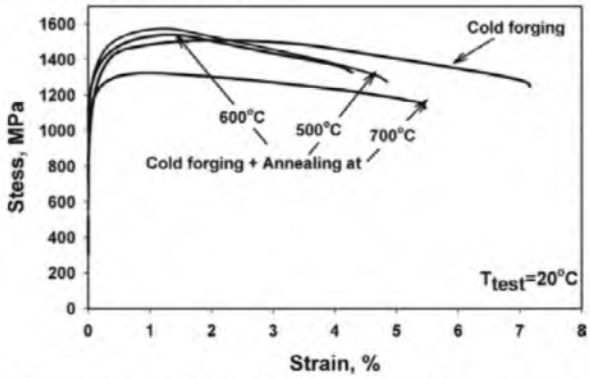


**Fig. 9.** Tensile stress-strain curves for a 304-type austenitic stainless steel processed by multiple forging to a total strain of $\varepsilon = 4$ and then annealed for 30 min at indicated temperatures.

and annealed steel are shown in Fig. 9. The specimens subjected to multiple forging to a total strain of 4 demonstrate high tensile strength above 1500 MPa. Annealing at temperatures of 500-600 °C is not accompanied by a remarkable softening; the level of tensile flow stress remains the same (Table 1). Such behaviour is closely related to the annealing effect on the microstructure. Since the main structural parameters do not change during annealing at temperatures of $T \leq 600$ °C, the tensile behaviours of the cold worked and annealed samples are the same. On the other hand, annealing at 700 °C is accompanied by a grain coarsening. Correspondingly, the tensile flow stress decreases as compared to the cold worked state. The structural investigations suggest that the softening is associ-

**Table 1.** The yield strength (YS), the ultimate tensile strength (UTS), and the elongation of the 304-type austenitic stainless steel after multiple forging to a total strain of 4 and annealing for 30 min at different temperatures.

| Property | Cold forging | 500 °C | 600 °C | 700 °C |
|---|---|---|---|---|
| YS, MPa | 1430 | 1420 | 1410 | 1190 |
| UTS, MPa | 1538 | 1570 | 1530 | 1320 |
| Elongation, % | 7.2 | 4.8 | 3.6 | 5.6 |

ated with a decrease in the dislocation density and an increase in the grain size.

## 4. SUMMARY

The structural changes and the mechanical properties were studied in a Super304H austenitic stainless steel subjected to large strain cold forging and subsequent annealing. The main results can be summarized as follows:

1. The multiple compressions of a 304-type austenitic stainless steel to a total strain of 4.0 results in the development of uniform nanocrystalline structure consisting of ferrite and austenite grains with a size of about 30 nm.
2. The evolution of the nano-grained microstructure is facilitated by the development of multiple mechanical twinning and strain-induced martensitic transformation.
3. The evolved microstructure is rather stable during the subsequent annealing at temperatures up to 600 °C, when a static recovery leads to a decrease in the dislocation density.
4. The heating to 700 °C results in the development of static recrystallization. The average recrystallized grain size is 500 nm after 30 min annealing.
5. The nanocrystalline steel processed by multiple forging exhibits high yield strength of 1430 MPa. Annealing for 30 min at temperatures below 600 °C does not lead to remarkable softening. The yield strength decreases to 1190 MPa only after annealing at 700 °C.

## ACKNOWLEDGEMENTS

This study was supported by Ministry of Education and Science, Russia, under grant No. 14.740.11.0333. Authors are grateful to the personnel of the Joint Research Center, Belgorod State University, for their assistance with instrumental analysis.

## REFERENCES

[1] F.J. Humphreys, P.B. Prangnell, J.R. Bowen, A. Gholinia and C. Harris // *Phil. Trans. R. Soc. Lond.* **357** (1999) 1663.

[2] R.Z. Valiev, R.K. Islamgaliev and I.V. Alexandrov // *Prog. Mater. Sci.* **45** (2000) 103.

[3] M. Tikhonova, A. Belyakov and R. Kaibyshev // *Mater. Sci. Forum* **706-709** (2012) 2326.

[4] J. Richert and M. Richert // *Aluminium* **62** (1986) 604.

[5] Y. Saito, N. Tsuji, H. Utsunomiya, T. Sakai and R.G. Hong // *Scr. Mater.* **39** (1998) 1221.

[6] I. Saunders and J. Nutting // *Met. Sci.* **18** (1984) 571.

[7] C.C. Koch // *Nanostr. Mater.* **9** (1997) 13.

[8] Y. Iwahashi, Z. Horita, M. Nemoto and T.G. Langdon // *Acta Mater.* **45** (1997) 4733.

[9] A. Belyakov, T. Sakai, H. Miura and K. Tsuzaki // *Phil. Mag. A* **81** (2001) 2629.

[10] S. Takaki, T. Tsuchiyama, K. Nakashima, H. Hidaka, K. Kawasaki and Y. Futamura // *Met. Mater. Int.* **10** (2004) 533.

[11] N. Tsuji, In: *Severe Plastic Deformation*, ed. by A. Burhanettin (Nova Science, New York, NY, 2005), p. 543.

[12] R.Z. Valiev, Y. Estrin, Z. Horita, T.G. Langdon, M.J. Zehetbauer and Y.T. Zhu // *JOM* **58** (2006) 33.

[13] C. Kobayashi, T. Sakai, A. Belyakov and H. Miura // *Phil. Mag. Lett.* **87** (2007) 751.

[14] A.P. Zhilyaev, A.A. Gimazov, G.I. Raab and T.G. Langdon // *Mater. Sci. Eng. A* **486** (2008) 123.

[15] A. Belyakov, Y. Kimura, Y. Adachi and K. Tsuzaki // *Mater. Trans.* **45** (2004) 2812.

[16] A. Belyakov, Y. Kimura and K. Tsuzaki // *Acta Mater.* **54** (2006) 2521.

[17] A. Belyakov, M. Murayama, Y. Sakai, K. Tsuzaki, M. Okubo, M. Eto and T. Kimura // *Journal of Electronic Materials* **35** (2006) 2000.

[18] S.V. Zherebtsov, G.S. Dyakonov, A.A. Salem, S.P. Malysheva, G.A. Salishchev and S.L. Semiatin // *Mater. Sci. Eng. A* **528** (2011) 3474.

[19] R.D.K. Misra, Z. Zhang, P.K.C. Venkatasurya, M.C. Somani and L.P. Karjalainen // *Mater. Sci. Eng. A* **527** (2010) 7779.

[20] S. Zherebtsov, M. Murzinova, G. Salishchev and S.L. Semiatin // *Acta Mater.* **59** (2011) 4138.

[21] A. Belyakov, K. Tsuzaki and R. Kaibyshev // *Mater. Sci. Forum* **667-669** (2011) 553.